View metadata, citation and similar papers at core.ac.uk
brought to you by CORE
provided by Open Archive Toulouse Archive Ouverte

Open Archive Toulouse Archive Ouverte (OATAO)

OATAO is an open access repository that collects the work of Toulouse researchers and makes it freely available over the web where possible.

This is an author-deposited version published in: http://oatao.univ-toulouse.fr/
Eprints ID : 2448

To link to this article :
URL : http://dx.doi.org/10.1149/1.2769265

To cite this version : Delmas, Mathieu and Vahlas, Constantin (2007) *Microstructure of Metallorganic Chemical Vapor Deposited Aluminum Coatings on Ti6242 Titanium Alloy.* Journal of The Electrochemical Society (JES), vol. 154 (n° 10). D538-D542. ISSN 0013-4651

Any correspondence concerning this service should be sent to the repository administrator: staff-oatao@inp-toulouse.fr

Microstructure of Metallorganic Chemical Vapor Deposited Aluminum Coatings on Ti6242 Titanium Alloy

Mathieu Delmas and Constantin Vahlas[*,z]

Centre Interuniversitaire de Recherche et d'Ingénierie des Matériaux (CIRIMAT–CNRS–INPT-UPS), ENCIACET, 31077 Toulouse Cedex 4, France

Al-based alloys are used in aeronautics as a protective layer against the excessive oxidation of turbines blades. In this work, Al coatings were deposited by metallorganic chemical vapor deposition on Ti6242, a commercial titanium alloy, with Pt as a sublayer or codeposited to ensure this protection, eventually forming platinum aluminides. Continuous Al coatings were deposited on bare Ti6242, using both triisobutylaluminum and dimethylethylamine alane as precursors. The same operating conditions applied on a platinum sublayer lead to discontinuous layers mainly containing whiskers. The introduction of a surfactant, namely, ethyl iodide, in the input gas improves the coating morphology by providing nearly whisker-free continuous films, suitable for oxidation protection. Codeposition of Pt and Al results in reduced growth rate and yields layers with lower Pt content and with specific morphology. This behavior is attributed to the competition between Al and Pt compounds on the growing surface.
DOI: 10.1149/1.2769265

Ti6242 titanium alloy is a promising material for the manufacturing of helicopter turbine components submitted to moderate stresses. In addition to titanium, it contains aluminum, tin, zirconium and molybdenum. The four digits in the Ti6242 code name refer to the wt % of these elements, respectively. This alloy is mainly composed of an α phase and of a low amount of a β phase, the latter being stabilized in ambient temperature by the abovementioned elements. It can be used at operating temperatures up to 823 K, provided it is protected against cyclic oxidation. Such protection can be conferred by Al-containing coatings which are widely used in the aeronautic industry, mainly as bond coats to prevent parts such as turbine blades and vanes from excessive oxidation. Al-containing coatings are mainly processed by the classical pack aluminization technique. Despite its simplicity, pack aluminization presents several drawbacks among which are powders disposal or high temperature operation. Considering that microstructural integrity and hence appropriate performance of the Ti6242 alloy is maintained only up to 873 K, the latter drawback prevents pack aluminization from being used for the application of protective coatings to this material. Unlike pack aluminization, metallorganic chemical vapor deposition (MOCVD) is not concerned by powders disposal; it operates at low to moderate temperature and yields highly conformal films. We recently presented a study on the MOCVD of pure and Pt-alloyed Al coatings on Ti6242 coupons.[1,2] Operating conditions for the MOCVD, preliminary characterization of the microstructure of the coatings and oxidation kinetics were reported. Isothermal oxidation of Ti6242 coupons covered by MOCVD processed Al coatings revealed noticeable protection with more than one order of magnitude lower oxidation kinetics than that of the bare alloy.[1] It was thus demonstrated that MOCVD is a promising alternative to the pack-aluminization technique.

However, the reported oxidation kinetics was characterized by an initial strong transient regime which was partially attributed to the rough microstructure of the coatings. It was concluded that more accurate control of the coating microstructure would be necessary for further decrease of both transient and steady state oxidation rate of the coated parts. This is the aim of the present paper. The MOCVD of Al films has been extensively studied for microelectronic applications (see, for example, Ref. 3) with particular focus on the improvement of their microstructure.[4,5] However, the constraints on the process and film characteristics are depending upon the aimed application. While microelectronics is concerned with reducing the thickness of the films, protective coatings should be continuous and several micrometers thick, and be applied on various commercial alloys or predeposited layers with industrial surface roughness. Also, protective coatings are often composed of two or more elements and the microstructure of the main element can be strongly influenced by the presence of the other(s). This is the case of the present study where Al is deposited on a Pt sublayer or codeposited with Pt. The pure Pt deposition will be described in a forthcoming paper. The microstructures of Al films regarding the nature of the substrate will be discussed in this study. The improvement of the rough microstructures obtained from deposition on Pt precoated substrates via the use of surfactants will be discussed, regarding surface chemistry phenomena. Finally, the simultaneous deposition of Al and Pt will be described. The particularities of such a codeposition will be illustrated and discussed.

Experimental

Depositions were performed on 2 mm thick, 15 mm diam Ti6242 disks. Substrates were used as received, i.e., with 600 grit surface polishing. Prior to deposition, they were etched in boiling Turco, cleaned ultrasonically in deionized water and finally degreased in acetone. Some disks were coated with a Pt film before Al deposition. A specially designed setup (the detailed description of the setup can be found in Ref. 2) was used for the CVD experiments. It allowed entire coating of coupons in a single run. It is recalled here that it consists in a vertical cold wall reactor in which the sample is maintained vertically by the two wires of an S-type thermocouple. Temperature is monitored by using a dual-wavelength pyrometer (Williamson), with $\pm 1°$ accuracy. Triisobutylaluminum (TIBA, 95% pure, Strem Chemicals), 99% pure dimethylathylamine alane (DMEAA, EPICHEM), and 99% pure trimethylmethylcyclopentadienylplatinum(IV) $[(MeCp)Me_3Pt]$ (Strem Chemicals) were used as liquid aluminum and platinum precursors, respectively, without further purification. TIBA and DMEAA are aluminum precursors yet widely used in microelectronics.[4,6] Decomposition of $[(MeCp)Me_3Pt]$, in the presence of H_2 was reported to provide essentially pure platinum films.[7]

The precursors' bubblers were loaded into a glove box. They were immersed in thermoregulated water baths to ensure fixed vapor pressure and, together with the flow rate of the bubbling gas, to control the compounds' molar fraction in the gas mixture entering the reactor. Three 99.998% pure N_2 lines were used: two for bubbling through the Al and Pt precursors and one for the dilution of the input gas. Before entering the reactor, the dilution line was combined with a 99.999% pure H_2 line for Pt deposition. Gases through all four lines were fed through computer driven mass flow controllers. The gas inlet circuit was made of stainless steel and wrapped with heating elements both before and after the bubblers to ensure efficient gas-liquid contact in the bubblers and to avoid premature condensation of the precursors. The gas phase was evacuated at the exit of the reactor by a vacuum pump via a cold trap. Operating pressure was 9330 Pa for deposition from TIBA and 1330 Pa for

[*] Electrochemical Society Active Member.
[z] E-mail: constantin.vahlas@ensiacet.fr

Table I. Operating conditions for the deposition of Al using TIBA and DMEAA.

Sample	Flow rate (sccm)				Reactor		
	$N_{2,dil.}$	$N_{2,Pr}$	Prec.	C_2H_5I	T (K)	P (Pa)	t (min)
AlT1	300	56.6	0.3654	No	623	9330	120
AlT2	300	56.6	0.3654	No	623	9330	120
AlT3	300	56.6	0.3654	Yes	623	9330	120
AlD1	41	3.15	0.1905	Yes	473	1330	75
AlD2	41	2.82	0.1704	Yes	473	1330	70

Table II. Operating conditions for the codeposition of Al and Pt.

Sample	Flow rate (sccm)						Reactor		
	$N_{2,dil.}$	$N_{2,Al.}$	DMEAA	$N_{2,Pt.}$	$Me_3(MeCp)Pt$	C_2H_5I	T (K)	P (Pa)	t (min)
AlPt1	40.5	1.8	0.0433	9	0.0242	Yes	473	1330	120
AlPt2	40.5	1.8	0.0433	9	0.0242	Yes	523	1330	120

deposition from DMEAA and codeposition. These values are higher than those reported in previous studies for the CVD of Al. They are compatible with the aimed industrial application. Cu and Al CVD deposited films present similar morphological characteristics, due to a Volmer-Weber growth mode.[8] It was reported that the use of ethyl iodide as a surfactant improves copper deposition. Ethyl iodide adsorbs dissociatively upon Al surfaces in the same way as on Cu surfaces.[9,10] Subsequently, we used iodine as a surfactant during Al deposition upon Pt. This was achieved by introducing a small amount of ethyl iodide in the gas phase during deposition. Tables I and II sum up the conditions used for the films deposition.

Surface and cross section scanning electron microscopy (SEM), transmission electronic microscopy (TEM), X-ray energy dispersive spectroscopy (EDS), grazing incident X-ray diffraction (GIXRD), interferometry, and atomic force microscopy (AFM) were used to investigate the morphology, microstructure, composition, surface topography, and roughness of the coatings.

Results

Figure 1 presents the AlT1 (a) and the AlD1 (b) samples surface. All SEM micrographs were realized at similar magnifications. Films obtained upon bare Ti6242 using TIBA (sample AlT1) present a continuous base and surface characteristics of Al crystals.[3] The average roughness of AlT1 is 1.7 μm. No preferential orientation could be observed with GIXRD analysis, and the carbon contamination is lower than 1 wt %. Observation of micrograph 1b reveals that the DMEAA based process (involving lower deposition temperature) leads to similar but finer microstructure than the TIBA based one.

Figure 2 presents the Arrhenius plot of DMEAA deposition on bare Ti6242 at 1330 Pa. From this diagram, activation energy of 0.3 eV was measured. The DMEAA processed coating, AlD1, exhibits an average roughness of 0.5 μm and a continuous base similar with results found by Vahlas et al.[11] Neither preferential orientation nor carbon contamination could be observed in AlD1.

Sample AlT2 corresponds to Al growth on Pt sublayer in the same conditions as for sample AlT1; it results in the formation of whiskers instead of continuous film. This microstructure does not present any significant continuous zone. Deposition from DMEAA results in a similar morphology. It is clear that such a discontinuous, rough morphology cannot meet the expected property from these coatings, namely the protection of the substrate against oxygen ingress.

Figure 3 presents surface (a) and cross section (b) SEM micrographs of sample AlT3. The microstructure of this coating consists of small crystals and only few surface whiskers. This morphology surmounts a continuous Al layer, illustrated in the cross section micrograph.

Figure 4 presents the SEM micrograph of the surface morphology (a) and the TEM cross section focusing on the area by the Pt sublayer, of sample AlD2; i.e., processed from DMEAA on Pt, by using C_2H_5I. Film AlD2 presents small sharp crystals whose shape is different from those observed on AlD1 and has no whiskers. The film is continuous and was processed at a growth rate of 1 μm/h. The 300 nm thick Pt sublayer appears as a black, compact strip. AFM measurements prior to Al deposition reveal that it is smooth and covers conformally the surface of the substrate. In addition, this Pt film did not show any scaling or peeling after deposition, even on a mirror-like, 1 μm polished substrate. A crystalline continuous Al film can be observed on the platinum film. The inset on this figure

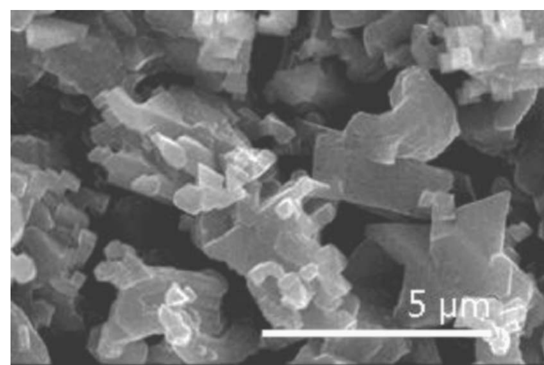

(a)

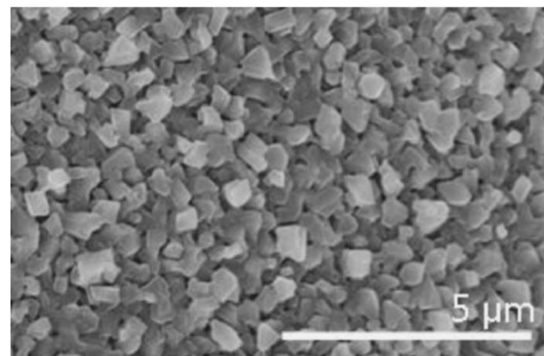

(b)

Figure 1. Surface SEM micrographs of samples AlT1 (a) and AlD1 (b): Al deposited on bare Ti6242 using TIBA and DMEAA, respectively.

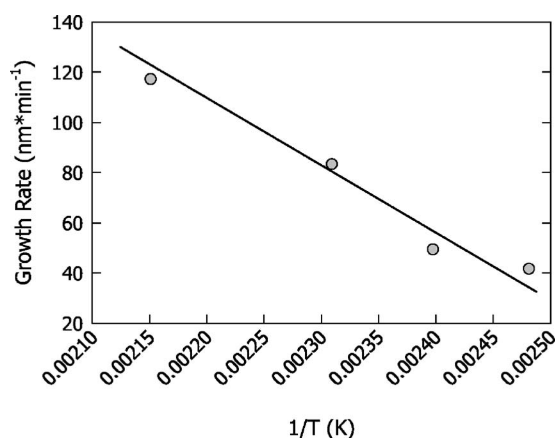

Figure 2. Arrhenius plot for the deposition of Al from DMEAA at 1330 Pa.

points out the Pt–Al interface. A 50 nm thick interdiffusion zone is shown to be developed during the deposition of Al; i.e., after 70 min at 473 K. The Pt/Al interface is very reactive,[12] the diffusion rate of Pt into Al being several orders of magnitude higher than that of Al into Pt.[13] The result of this phenomenon is the formation of platinum aluminides and especially Al_2Pt. It thus appears that, as for TIBA processed samples, ethyl iodide assisted Al deposition from DMEAA on Pt provides continuous films. Both TIBA and DMEAA processed films show very low C contamination (less than 1 wt %) and no preferential orientation. Iodine contamination of the surfactant assisted films remains under 1 wt %.

Al–Pt codeposition in conditions AlPt1 corresponds to a growth rate of ~1 μm/h. This value is low compared with the calculated

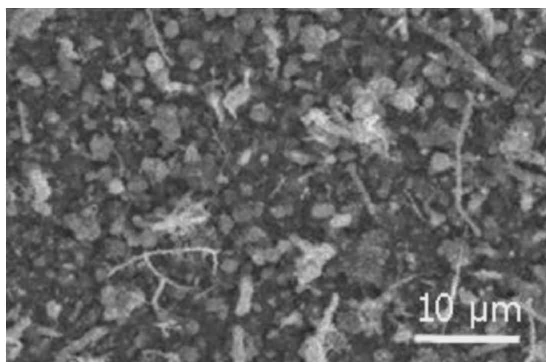

(a)

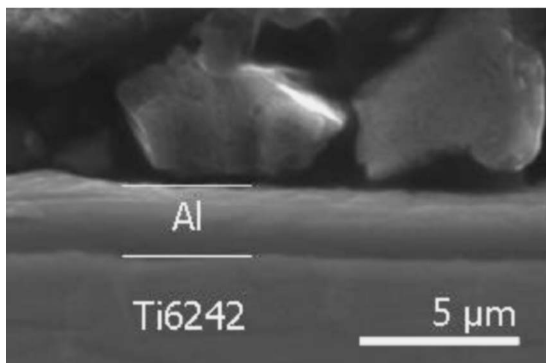

(b)

Figure 3. Surface (a) and cross section (b) SEM micrographs of sample AlT3: I-assisted Al deposition on Pt using TIBA.

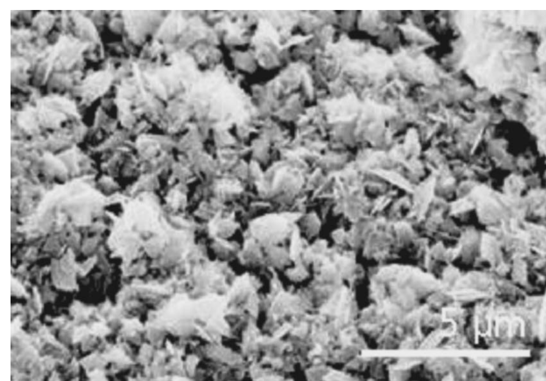

(a)

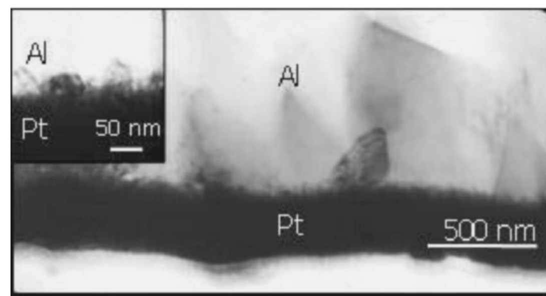

(b)

Figure 4. Surface SEM micrograph (a) and cross section TEM micrograph with detail of the Al–Pt interface (b) of sample AlD2: Al deposited on Pt using DMEAA with surfactant.

growth rates of Al (6 μm/h) and Pt (1 μm/h) in the same conditions. Figure 5 presents a surface SEM micrograph of such a film, processed for 2 h. The Ti6242 surface roughness can be observed thus confirming the conformality and the reduced thickness of the film.

Figure 6 presents a SEM micrograph of the AlPt2 surface. This coating consists of a codeposition performed at 523 K, with a resulting growth rate of 6 μm/h. It can be noticed that the microstructure is close to that of the 473 K processed codeposited sample. AlPt2 presents a higher average roughness of 240 nm and does not show any carbon contamination. The Pt content is about 16 wt %, still lower than the Pt molar fraction in the gas phase, but significantly higher than that of the 473 K deposited coatings.

Despite the low processing temperature, GIXRD patterns of samples AlPt1 and AlPt2 indicate that both films are composed of

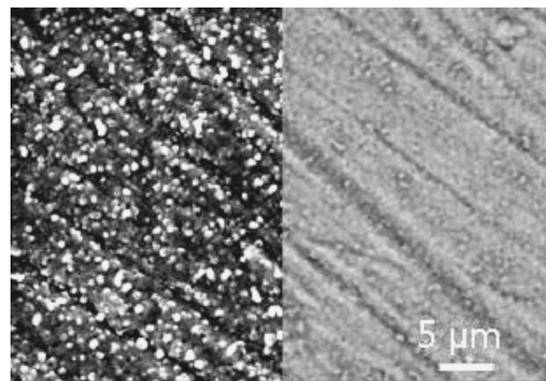

Figure 5. Secondary (left) and backscattered (right) electrons surface SEM micrographs of sample AlPt1: Al and Pt codeposited on Ti6242 at 473 K.

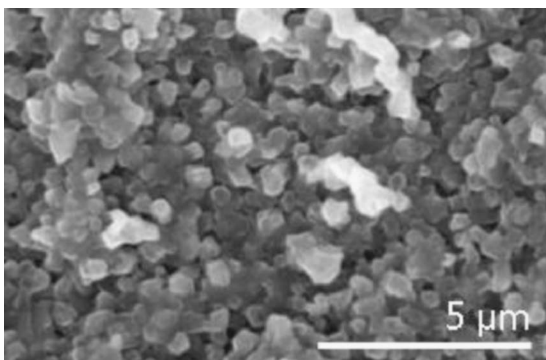

Figure 6. Surface SEM micrograph of sample AlPt2: Al and Pt codeposited on Ti6242 at 523 K.

Al, with several Al–Pt compounds, such as $PtAl_2$, $Al_{21}Pt_8$, $Al_{21}Pt_6$, Pt_2Al. No preferential orientation could be observed in Al.

Discussion

Vahlas et al.[11] reported that MOCVD processed Al coatings from TIBA on silicon carbide strongly depend on surface pretreatments. Deposition on Ti6242 is more straightforward as nucleation is easier on metallic surfaces. DMEAA allows deposition on Ti6242 of continuous films without pretreatments, as well. The activation energy of DMEAA processed Al coatings on Ti6242 (0.3 eV) is consistent with those reported in the literature (between 0.1 and 0.7 eV, depending on the substrate).[14-17] However, DMEAA seems to be very sensitive to the nature of the substrate. Jang et al. demonstrated that a better conductivity of the substrate decreases the activation energy.[14] The value determined by Jang for conductive substrates (TiN) is three times lower than the one estimated in the present work. However, other studies using Si as a substrate indicate higher values than Jang's ones,[15,16] and modeling of DMEAA decomposition on Al surface resulted in $E_a = 0.3$ eV;[17] it can thus be concluded that this is an accurate value for activation energy on metallic surfaces.

The loose microstructure of the AlT2 sample can be linked to the catalytic properties of Pt. Deposition of Al from TIBA can lead spontaneously to the formation of whiskers, as described by Zhuk et al.[18] The obtained whiskers are rather thick (—a few hundreds nanometers in diameter—) and present many bends but no branching. This behavior has been observed on Ti6242, as well. This growth mode is due to adsorption on the Al surface of precursor ligands leading to volatile compounds with Al adatoms. Surface mobility of those compounds allows their concentration on preferential sites where they are decomposed, forming the growing whiskers. This whiskers growth mechanism seems to be enhanced by the Pt sublayer. Whiskers appearing then are thinner and branched (sample AlT2). It has been reported that co-adsorption of ferrocene on the surface prevents such a behavior through the blocking action of the adsorbed cyclopentadienyl groups.[18] These adsorbed cyclopentadienyl groups seem to prevent such behavior, avoiding then the whiskers growth. However, this solution could not be applied here, because of the resulting undesirable Fe contamination. On the other hand, copper deposition encounters rough and discontinuous microstructures. As has already been mentioned, the use of surfactant, namely C_2H_5I, allows to achieve continuous and smoother films.[8] It has been reported that alkyliodides are dissociatively adsorbed on Al surfaces, with the C–I bond breaking since 200 K.[9] According to Tölkes et al.,[17] the iodine atoms may act in two ways. First, by lowering the surface energy of the system, the balance between the activation energies for nucleation and for growth of Al is shifted towards the nucleation, this resulting in surface smoothening. Second, the presence of I lowers the Ehrlich-Schwoebel barrier, i.e., the energy barrier responsible for the diffusion of adatoms across the atomic steps. Diffusion of the adatoms through atomic steps is then improved again, allowing the growth of a smoother surface. Based on these mechanisms, addition of a C_2H_5I stream in the dilution gas during deposition leads to coatings presenting a continuous base. Al films grown on Pt using DMEAA and surfactant assistance also yield continuous and whisker-free morphology (Fig. 4). As I presents an atomic radius far larger than that of Al, and is a low surface-energy element, it segregates at the surface during the growth and results in no significant contamination, as was attested by EDS.

The mechanisms of Al and Pt codeposition are different from those prevailing for single elements. However, due to the lack of in situ observations, we can only make several assumptions. Pt deposition using $Me_3(MeCp)Pt$ presents an induction period followed by an autocatalytic growth.[7] The autocatalytic growth appears when the Pt clusters' size allows the catalytic properties to appear. During codeposition, Al growth prevents Pt atoms from forming clusters. The deposition rate of platinum drops dramatically. The reduced concentration of Pt in the films is attributed to this phenomenon. The shift of growth rate to higher temperature indicates further interactions between the two precursors. According to Nakajima et al.,[17] DMEAA decomposes in dimethylethylamine and alane while approaching the surface. Two possibilities can be foreseen for the interaction between the alane and the Pt precursor: First, alane would react rapidly with the Pt precursor in the gas phase thus reducing the availability of the latter in the deposition process. Second, the alane would adsorb on the substrate, with the Al atom first. As the Pt precursor coordinates to the surface through the cyclopentadienyl ligand,[7,19] this ligand may remain at the aluminum surface. The work of Zhuk et al. enlightens the influence of such an adsorption on Al film growth.[18] This phenomenon results in the decrease of the growth rate of Al and ultimately of the film, since Al is the major component of the latter. Moreover, it is worth noting that the area of an adsorbed cyclopentadienyl on a Pt (111) surface is about ten times larger than that of Al.[6,19] This difference can also explain to a certain extent the morphological perturbation of Al films in the presence of $Me_3(MeCp)Pt$.

The above observed microstructures can be correlated to the performance of the as processed oxidation barriers. Thermogravimetric tests were performed in dry air on such processed samples, with the test conditions and the obtained results reported in Ref. 1. The link between samples' morphology and oxidation behavior was established and quantified through the parabolic rate constant of oxidation kinetics, k_p ($mg^2\ cm^{-4}\ s^{-1}$), determined by plotting the mass gain vs square root of time.[20] It is recalled that sample AlT1 yields no reduction of the k_p compared with the bare alloy. Also, in the same test conditions samples AlD2 and AlPt2 showed an improvement of the oxidation protection, resulting in a k_p ten times lower than that of the bare alloy. This improvement can be attributed to the compactness of these films and their smoother surface morphology with regard to films processed in conditions AlT1.

Conclusion

The deposition of several micrometers thick Al by MOCVD using TIBA and DMEAA on titanium alloy Ti6242 leads to films with a continuous base, no C contamination and no preferred orientation. The surface of such films is composed of Al crystals, smaller for DMEAA-processed films. When deposited on Pt sublayer in similar conditions, the deposits are mainly composed of very thin whiskers. By adding a C_2H_5I stream in the dilution gas, the obtained microstructure is whisker-free, continuous, with no texture. No C contamination could be detected, and I concentration remains at the EDS detection threshold. Simultaneous deposition of Pt and Al leads to Al coatings containing Pt–Al phases. A lower growth rate than those of single elements and an Al/Pt ratio in the films higher than the input gas phase are characteristics of the specific growth mechanism taking place during codeposition. Those interferences between decomposition mechanisms and coatings characteristics can be explained by competitive adsorption at the growing surface and the difference between the Al and Pt catalytic behaviors. The direct

relations between the microstructure of the deposited coatings and the properties of use, namely protection against oxidation, have been illustrated.

Acknowledgments

The authors are indebted to Yolande Kihn, CEMES, for TEM observations. This work is part of the APROSUTIS project supported by the Réseau National Matériaux et Procédés (RNMP) network (Ministère de la Recherche, opération 02 K0298). It was performed through a grant to M.D. from the French Ministry of Education.

Centre National de la Recherche Scientifique assisted in meeting the publication costs of this article.

References

1. M. Delmas, D. Poquillon, C. Vahlas, and Y. Kihn, *Surf. Coat. Technol.*, **200**, 1413 (2005).
2. M. Delmas, M. Ucar, L. Ressier, M. Pons, and C. Vahlas, *Surf. Coat. Technol.*, **188–189**, 49 (2004).
3. T. Kodas, M. G. Simmonds, and W. L. Gladfelter, in *The Chemistry of Metal CVD*, T. T. Kodas, M. Hampden-Smith, Editors, p. 45 VCH, (1994).
4. R. Jonnalagadda, D. Yang, B. R. Rogers, J. T. Hillman, R. F. Foster, and T. S. Cale, *J. Mater. Res.*, **14**, 1982 (1999).
5. K. Sugai, H. Okabayashi, S. Kishida, and T. Shinzawa, *Thin Solid Films*, **280**, 142 (1996).
6. W. L. Gladfelter and E. C. Phillips, U.S. Pat. (1991).
7. Z. Xue, H. Tridandam, H. D. Kaesz, and R. F. Hicks, *Chem. Mater.*, **4**, 162 (1992).
8. E. S. Hwang and J. Lee, *Electrochem. Solid-State Lett.*, **3**, 138 (2000).
9. B. E. Bent, R. G. Nuzzo, and L. H. Dubois, *J. Am. Chem. Soc.*, **111**, 1634 (1989).
10. B. E. Bent, R. G. Nuzzo, B. R. Zegarski, and L. H. Dubois, *J. Am. Chem. Soc.*, **113**, 1137 (1991).
11. C. Vahlas, P. Ortiz, D. Oquab, and I. W. Hall, *J. Electrochem. Soc.*, **148**, C583 (2001).
12. E. G. Colgan, *J. Appl. Phys.*, **62**, 1224 (1987).
13. P. Gas, J. Labar, G. Clugnet, A. Kovacs, C. Bergman, and P. Barma, *J. Appl. Phys.*, **90**, 3899 (2001).
14. T. W. Jang, H. S. Rhee, and B. T. Ahn, *Mater. Res. Soc. Symp. Proc.*, **514**, 351 (1998).
15. H. Matsuhashi, C.-H. Lee, T. Nishimura, K. Masu, and K. Tsubouchi, *Mater. Sci. Semicond. Process.*, **2**, 303 (1999).
16. Y. Neo, M. Niwano, H. Mimura, and K. Yokoo, *Appl. Surf. Sci.*, **142**, 443 (1999).
17. T. Nakajima, M. Nakatomi, and K. Yamashita, *Mol. Phys.*, **101**, 267 (2003).
18. B. V. Zhuk and V. K. Khamylov, Dokl. Akad. Nauk, **233**, 862 (1977).
19. N. R. Avery, *Surf. Sci.*, **146**, 363 (1984).
20. D. Monceau and B. Pieraggi, *Oxid. Met.*, **50**, 477 (1998).